

# Miscible Crystalline/Crystalline Polymer Blends of Poly(vinylidene fluoride) and Poly(butylene succinate-*co*-butylene adipate): Spherulitic Morphologies and Crystallization Kinetics<sup>†</sup>

Zhaobin Qiu,\* Chunzhu Yan, Jiaoming Lu, and Wantai Yang

State Key Laboratory of Chemical Resource Engineering, Beijing University of Chemical Technology, Beijing 100029, China

Received January 29, 2007; Revised Manuscript Received April 4, 2007

**ABSTRACT:** Spherulitic morphologies and overall crystallization kinetics of miscible poly(vinylidene fluoride) (PVDF)/poly(butylene succinate-*co*-butylene adipate) (PBSA) blends were studied by polarizing optical microscopy (POM), differential scanning calorimetry (DSC), and wide-angle X-ray diffraction (WAXD). PVDF and PBSA crystallize separately in the blends. For the high- $T_m$  component PVDF, the crystallization mechanism does not change, while both the spherulitic growth rate and the overall crystallization rate of PVDF decrease with increasing crystallization temperature and the PBSA content in the blends. Much more attention has been directed to the spherulitic morphologies and overall crystallization kinetics of the low- $T_m$  component PBSA, which are affected not only by blend composition and crystallization temperature but also strongly by the preexisting crystals of the high- $T_m$  component PVDF in the blends. PBSA spherulites nucleate in the matrix of the PVDF spherulites and continue to grow until impinging on other PBSA spherulites. The overall crystallization rate of PBSA is accelerated in the blends compared with that of neat PBSA, which reduces with increasing crystallization temperature despite blend composition for the PBSA-rich blends. The presence of the preexisting PVDF crystals shows two opposite effects on the overall crystallization of PBSA, i.e., enhanced nucleation ability and slower crystal growth rates.

## Introduction

Miscibility and crystallization of polymer blends have been studied extensively. However, blends in which both components are crystalline polymers have received much less attention than fully amorphous or amorphous/crystalline systems. It is more complicated and interesting to investigate this special kind of blend of two crystalline polymers since both components are able to crystallize. Up to now, only a small number of works have been reported on miscible polymer blends of two crystalline polymers with different chemical structures.<sup>1–16</sup> However, they may provide various conditions to study the crystallization behavior and morphology of polymer blends. The difference in the melting point  $T_m$  of the two components plays a significant role of determining the crystallization and morphology when binary miscible crystalline/crystalline polymer blends crystallize from the homogeneous melt. When the difference in  $T_m$ s is large, the two components cannot crystallize simultaneously but separately.<sup>1–8</sup> However, the two components can crystallize simultaneously when the  $T_m$  difference is small.<sup>9–16</sup> Furthermore, interpenetrated spherulites are occasionally formed in a few miscible pairs of two crystalline polymers when the two components crystallize simultaneously.<sup>9–16</sup> Spherulites of one component continue to grow in the spherulites of the other component after they contact with each other. The interpenetrated spherulites formation processes have been found in poly-(3-hydroxybutyrate)/poly(L-lactide) (PLLA),<sup>9</sup> poly(butylene succinate) (PBSU)/poly(vinylidene chloride-*co*-vinyl chloride) (PVCVC),<sup>10–12</sup> poly(ester carbonate) (PEC)/PLLA,<sup>13,14</sup> poly(ethylene succinate) (PES)/poly(ethylene oxide) (PEO),<sup>15</sup> and PBSA/PEO blends.<sup>16</sup>

It should be noted that the crystallization and morphology of binary miscible crystalline polymer blends are far away from being really understood. Much more attention has been paid to the crystallization and morphology of the high- $T_m$  component in miscible crystalline/crystalline polymer blends until now; however, crystalline/crystalline polymer blends actually become crystalline/amorphous polymer blends when the high- $T_m$  component crystallizes at crystallization temperature above  $T_m$  of the low- $T_m$  component. Less attention has been paid to the crystallization and morphology of the low- $T_m$  component, which are actually affected not only by blend composition and crystallization temperature but also strongly by the preexisting crystals of high- $T_m$  component in the blends.

In this work we chose PVDF and PBSA as the model system of miscible crystalline/crystalline polymer blends. The miscibility of PVDF/PBSA blends was evidenced by the depression of crystallization peak temperature and melting point temperature of each component with increasing the content of the other component and the homogeneous melt.<sup>17</sup> The two polymers are both crystalline in their neat state, which undergo crystallization over a wide range of temperatures. Since the difference in the melting points between PVDF (ca. 165 °C) and PBSA (ca. 95 °C) is large, the simultaneous crystallization of the two components is impossible. The crystallization of PVDF corresponds to the transition from the fully amorphous to the amorphous/semicrystalline state. PBSA is still in the melt as an amorphous diluent throughout the crystallization of PVDF. On further lowering crystallization temperature, the crystallization of PBSA corresponds to the transition from the amorphous/semicrystalline to semicrystalline/semicrystalline state. PVDF always crystallizes during the quenching process before  $T_c$  of PBSA is reached, and PBSA must crystallize in the matrix of the preexisting PVDF crystals. In the present work spherulitic morphologies and crystallization kinetics of both components were studied by taking into account the influences of blend

\* Corresponding author: e-mail qiuqb@mail.buct.edu.cn, Fax +86-10-64413161.

<sup>†</sup> Dedicated to Dr. Toshio Nishi, emeritus professor of The University of Tokyo and professor of Tokyo Institute of Technology, on the occasion of his 65th birthday.

composition and crystallization temperature. Moreover, much more attention has been directed to the crystallization and morphology of the low- $T_m$  component PBSA by considering the effect of the presence of preexisting crystals of the high- $T_m$  component PVDF.

### Experimental Section

PVDF ( $M_w = 140\,000$ ) and PBSA ( $M_w = 14\,400$ ), a copolymer with 20 mol % butylene adipate, were purchased from Polysciences, Inc., and Aldrich Chemical Co., respectively. PVDF/PBSA blends were prepared with mutual solvent *N,N*-dimethylformamide (DMF). The solution of both polymers (0.02 g/mL) was cast on glass plate at an elevated temperature. The solvent continued to evaporate in a controlled air stream for 1 day. The resulting films were further dried in vacuum at 50 °C for 3 days to remove DMF completely. PVDF/PBSA blends were prepared with various compositions ranging from 100/0, 80/20, 65/35, 50/50, 35/65, 20/80 to 0/100 in weight ratio, the first number referring to PVDF.

Thermal analysis was performed using a TA Instruments differential scanning calorimetry (DSC) Q100 with a Universal Analysis 2000. The samples were first annealed at 190 °C for 3 min to erase any thermal history and cooled to -70 °C at 10 °C/min. The crystallization peak temperature ( $T_p$ ) was obtained from the DSC cooling traces. The isothermal crystallization of PVDF/PBSA blends was studied using the following processes. For the high- $T_m$  component PVDF, the sample was annealed at 190 °C for 3 min, cooled at 40 °C/min to the crystallization temperature ( $T_{c1}$ ) between  $T_m$ s of PVDF and PBSA, and then maintained at  $T_{c1}$  until the crystallization of PVDF completed. For the low- $T_m$  component PBSA, the sample was first crystallized at 120 °C ( $T_{c1}$ ) for 5 min for PVDF to finish crystallization and then cooled at 40 °C/min to the second crystallization temperature ( $T_{c2}$ ) below  $T_m$  of PBSA to for PBSA to finish isothermal crystallization. The aforementioned isothermal crystallization condition consists of the following two steps, namely, the isothermal crystallization of the PVDF phase at  $T_{c1}$  from the homogeneous melt and the isothermal crystallization of the PBSA at  $T_{c2}$  from the liquid phase in the presence of PVDF crystals previously formed at 120 °C.

A polarizing microscope (Olympus BX51) equipped with a first-order retardation plate and a temperature controller (Linkam THMS 600) was used to investigate the spherulitic morphology and growth of PVDF/PBSA blends. The spherulitic growth rate  $G$  was studied by following the variation of radius  $R$  against crystallization time  $t$ , i.e.,  $G = dR/dt$ .

Wide-angle X-ray diffraction experiments were performed on a Rigaku D/Max 2500 VB2+/PC X-ray diffractometer at 40 kV and 200 mA. The PVDF/PBSA blends samples were first pressed into films with thickness of around 1 mm on a hot stage at 190 °C for 3 min, transferred into one oven preset at 120 °C as soon as possible and held for 5 min for PVDF to finish crystallization, and then transferred into the other oven preset at 70 °C as soon as possible and held for 1 h for PBSA to finish crystallization. For neat components, PVDF only crystallized at 120 °C for 5 min while PBSA only crystallized at 70 °C for 1 h from the melt, respectively. It should be noted that the samples prepared for the WAXD measurements experienced the similar thermal history as those for the overall crystallization kinetics and spherulitic morphology studies by DSC and POM mentioned in the above section.

### Results and Discussion

**Separate Crystallization of PVDF/PBSA Blends.** PVDF has a  $T_m$  of 165 °C, while PBSA has a  $T_m$  of 95 °C. Because of the large difference in  $T_m$ s, it is impossible for the two components to crystallize simultaneously. Figure 1 shows the DSC cooling traces of PVDF/PBSA blends at 10 °C/min from the homogeneous melt. Neat PVDF shows a  $T_p$  at 136.6 °C, and neat PBSA has a  $T_p$  at 53.4 °C. The difference in  $T_p$ s between neat PVDF and PBSA is over 80 °C. Furthermore,  $T_p$  of PVDF shifts to low-temperature range with increasing the PBSA content in the

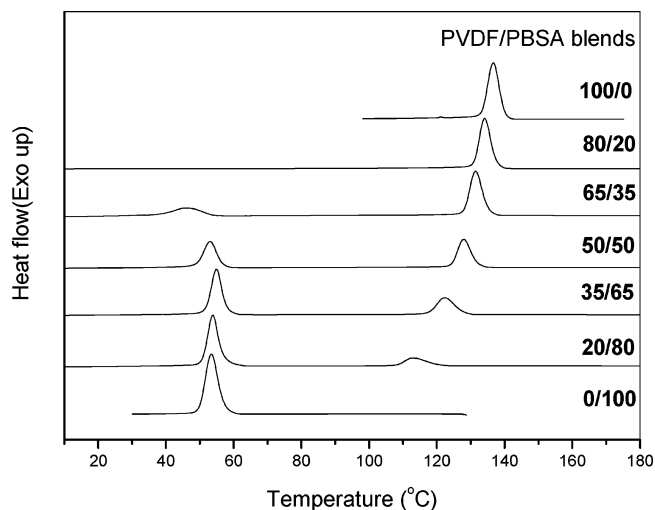


**Figure 1.** DSC traces of PVDF/PBSA blends cooled from the homogeneous melt at 10 °C/min.

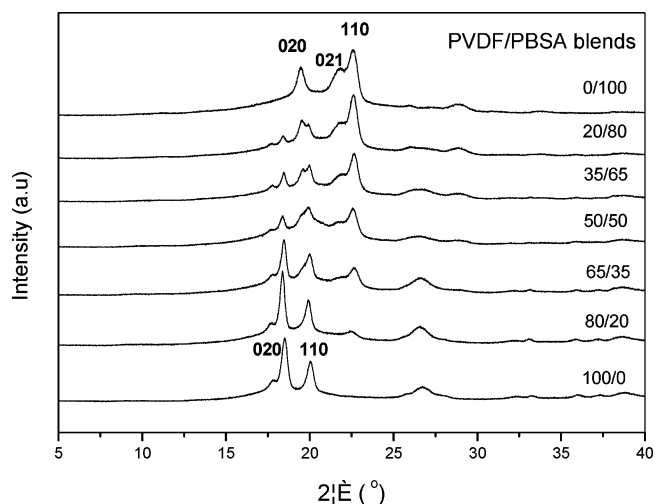


**Figure 2.** WAXD patterns of PVDF/PBSA blends.

blends.  $T_p$  of PVDF in the 20/80 blend is only around 112.7 °C, which is lower than that of neat PVDF by over 20 °C. On the other hand,  $T_p$  of PBSA is at around 54 °C and almost unchanged despite blend composition with increasing the PVDF content up to 50 wt %. However,  $T_p$  of PBSA decreases to 45.6 °C in the 65/35 blend with further increasing the PVDF content. Therefore, it is obvious that PVDF and PBSA do not crystallize simultaneously but crystallize separately in different temperature range.

In order to investigate the effect of blending another crystalline component on the crystal structure of one component, WAXD experiments of PVDF/PBSA blends were performed. Figure 2 demonstrates the WAXD patterns of PVDF/PBSA blends with various blend compositions. Neat PVDF shows two strong diffraction peaks at around 18.2° and 19.8° corresponding to (020) and (110) planes, respectively.<sup>18</sup> On the other hand, neat PBSA displays three strong diffraction peaks at around 19.3°, 21.5°, and 22.4° corresponding to (020), (021), and (110) planes, respectively.<sup>19,20</sup> The WAXD patterns involve all the diffraction peaks corresponding to neat components in the blends, and the intensity of the diffraction peaks of each component decreases with increasing the other component content. The WAXD results indicate again that PVDF and PBSA crystallize separately in the blends. Blending with another semicrystalline polymer does not modify the crystal structure in the blends but only reduces the intensity of diffraction peak.

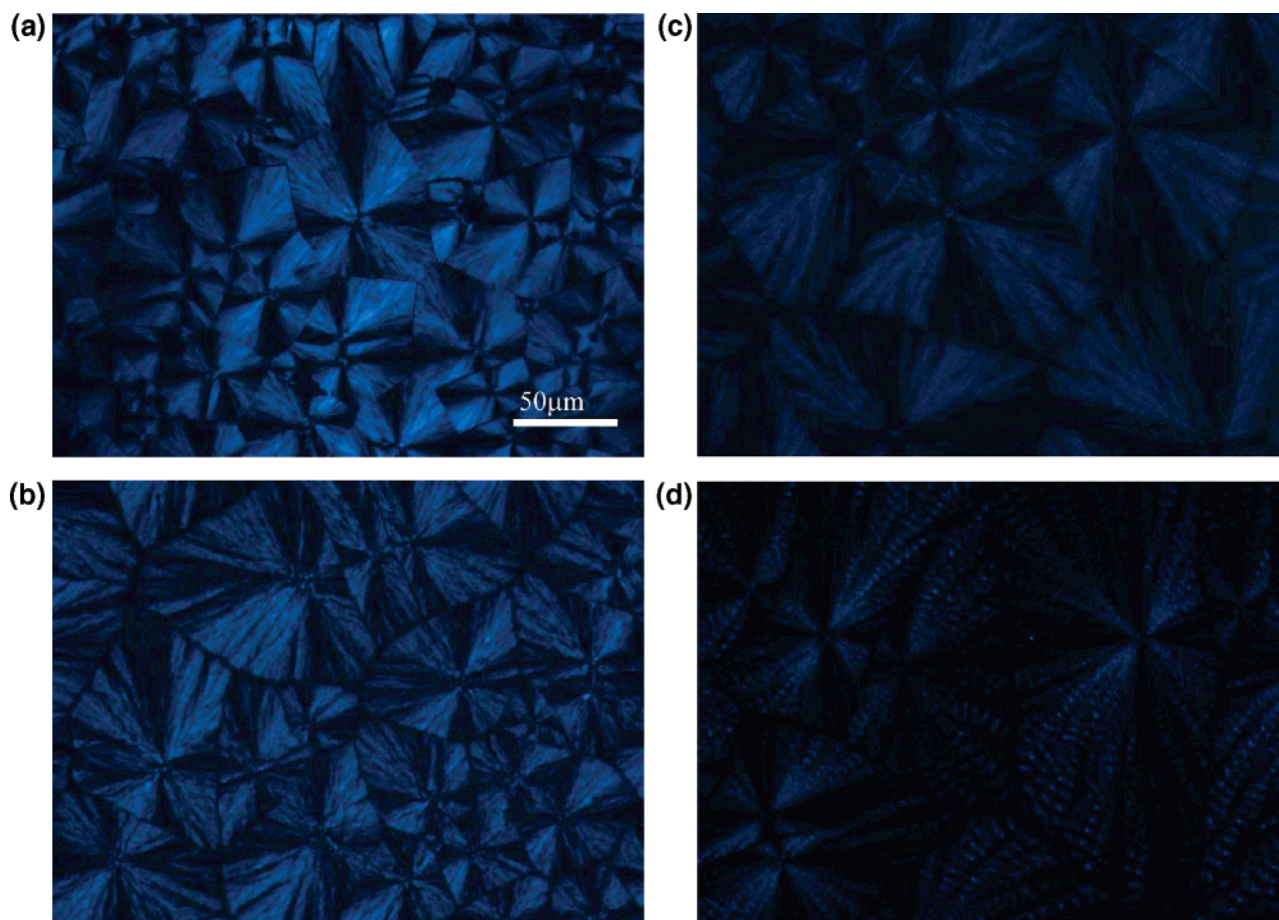


**Figure 3.** PVDF spherulites at 144 °C in the PVDF-rich blends (same magnification with bar = 50  $\mu\text{m}$ ): (a) 100/0 for 5 min, (b) 80/20 for 15 min, (c) 65/35 for 16 min, and (d) 50/50 for 30 min.

Therefore, it can be concluded that PVDF and PBSA crystallize separately in the blends on the basis of the DSC and WAXD results.

**Crystallization of High- $T_m$  Component PVDF.** PVDF/PBSA blends are miscible crystalline/crystalline polymer blends with PVDF being high- $T_m$  component and PBSA being low- $T_m$  component. PBSA is still in the melt when PVDF crystallizes at  $T_{c1}$ . Therefore, the crystallization of PVDF at  $T_{c1}$  from the homogeneous melt corresponds to the transition from the amorphous/amorphous to the amorphous/crystalline state. The spherulitic morphology and growth rate of the PVDF phase were studied with OM at different crystallization temperature for various blend compositions. Figure 3 presents the blend composition effect on the PVDF spherulitic morphologies at 144 °C. It is obvious that the PVDF spherulites become larger with increasing the PBSA content, indicative of the decrease of nucleation. Furthermore, banded PVDF spherulites are found for the PVDF/PBSA 50/50 blend (Figure 3d).

The spherulitic growth rate of PVDF was measured by following the variation of radius of spherulites against crystallization time. It was found that the spherulites grew linearly with time for both neat and blended PVDF in the investigated crystallization temperature range. Figure 4 summarizes the crystallization temperature and blend composition effects on the spherulitic growth rates of PVDF. The spherulitic growth rates decrease with increasing crystallization temperature despite blend compositions. On the other hand, the spherulitic growth rates decrease with increasing the PBSA content in the blends for a given crystallization temperature. The decrease in the spherulitic growth rates becomes more significant at low

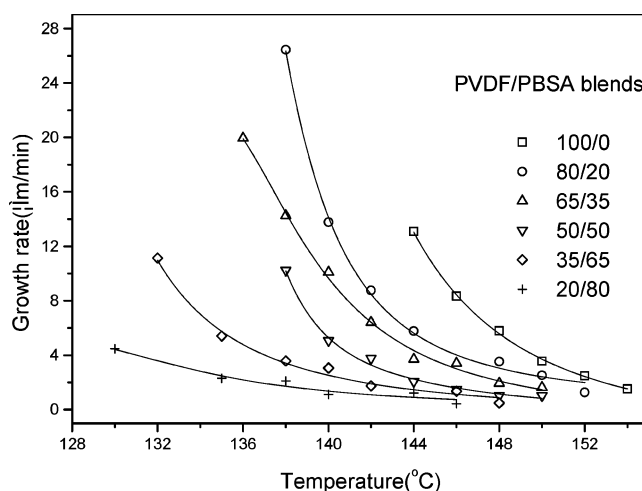


**Figure 4.** Temperature dependence of spherulitic growth rates of PVDF for the PVDF/PBSA blends.

crystallization temperature than at high crystallization temperature, indicating that the supercooling plays a dominant role of determining the spherulitic morphology and growth rates. The decrease of the spherulitic growth rates may be related to the following two factors. One is the depression of  $T_m$  of PVDF after blending with PBSA, which reduces the driving force for the crystallization process from the homogeneous melt. For example,  $T_m$  decreased from 165 °C for neat PVDF to 146.7 °C for the 20/80 blend. The other is that PBSA is still in the melt during the crystallization of PVDF and plays a diluent role during the growth process of PVDF spherulites. Therefore, it can be concluded that increasing the crystallization temperature



Table 1. Crystallization Kinetic Parameters of PVDF in the PVDF-Rich Blends

PVDF/PBSA blends	$T_c$ (°C)	$n$	$k$ (min <sup>-n</sup> )	$t_{0.5}$ (min)	$1/t_{0.5}$ (min <sup>-1</sup> )
100/0	144	2.6	$2.36 \times 10^{-1}$	1.51	$6.62 \times 10^{-1}$
	146	2.7	$5.64 \times 10^{-2}$	2.53	$3.95 \times 10^{-1}$
	148	2.6	$1.29 \times 10^{-2}$	4.52	$2.21 \times 10^{-1}$
	150	2.6	$2.16 \times 10^{-3}$	9.20	$1.09 \times 10^{-1}$
	152	2.6	$4.57 \times 10^{-4}$	16.7	$5.98 \times 10^{-2}$
80/20	140	2.4	$7.76 \times 10^{-1}$	$9.53 \times 10^{-1}$	1.05
	142	2.5	$2.19 \times 10^{-1}$	1.59	$6.29 \times 10^{-1}$
	144	2.4	$5.99 \times 10^{-2}$	2.85	$3.51 \times 10^{-1}$
	146	2.6	$9.84 \times 10^{-3}$	5.07	$1.97 \times 10^{-1}$
	148	2.5	$2.80 \times 10^{-3}$	9.15	$1.09 \times 10^{-1}$
65/35	136	2.5	1.84	$6.83 \times 10^{-1}$	1.46
	138	2.5	$4.06 \times 10^{-1}$	1.24	$8.06 \times 10^{-1}$
	140	2.4	$1.50 \times 10^{-1}$	1.90	$5.26 \times 10^{-1}$
	142	2.5	$3.01 \times 10^{-2}$	3.45	$2.90 \times 10^{-1}$
	144	2.4	$9.74 \times 10^{-3}$	5.83	$1.72 \times 10^{-1}$
50/50	134	2.5	1.26	$7.89 \times 10^{-1}$	1.27
	136	2.3	$4.94 \times 10^{-1}$	1.16	$8.62 \times 10^{-1}$
	138	2.4	$1.62 \times 10^{-1}$	1.86	$5.38 \times 10^{-1}$
	140	2.5	$6.12 \times 10^{-2}$	2.66	$3.76 \times 10^{-1}$
	142	2.5	$2.09 \times 10^{-2}$	4.18	$2.39 \times 10^{-1}$

and the PBSA content have the similar effects on the spherulitic morphology and growth of the PVDF phase in its miscible blends with PBSA.

The overall crystallization kinetics of PVDF was studied by DSC at various crystallization temperatures in the PVDF-rich blends. The well-known Avrami equation is used to analyze the isothermal crystallization kinetics; it assumes the development of the relative degree of crystallinity  $X_t$  with crystallization time  $t$  as

$$1 - X_t = \exp(-kt^n) \quad (1)$$

where  $n$  is the Avrami exponent depending on the nature of nucleation and growth geometry of the crystals, and  $k$  is a composite rate constant involving both nucleation and growth rate parameters.<sup>21</sup> In the case of the DSC experiment, the relative degree of crystallinity  $X_t$  at crystallization time  $t$  is defined as the ratio of the area under the exothermic curve between the onset crystallization time and the crystallization time  $t$  to the whole area under the exothermic curve from the onset crystallization time to the end crystallization time.

The half-life crystallization time  $t_{0.5}$ , the time required to achieve 50% of the final crystallinity of the samples, is an important parameter for the discussion of crystallization kinetics. Usually, the crystallization rate is easily described as the reciprocal of  $t_{0.5}$ . The value of  $t_{0.5}$  is calculated by the following equation:

$$t_{0.5} = (\ln 2/k)^{1/n} \quad (2)$$

where  $n$  and  $k$  are the same as in the Avrami equation.

Table 1 summarizes all the related crystallization kinetics parameters for the isothermal crystallization of PVDF in the PVDF-rich blends at various crystallization temperatures. The crystallization of PVDF is affected not only by crystallization temperature but also by blend composition in the blends. For a given crystallization temperature the values of  $t_{0.5}$  in the blends are larger than that of neat PVDF and become larger with increasing the PBSA content. On the other hand, the values of  $k$  and  $1/t_{0.5}$  in the blends are smaller than those of neat PVDF and become smaller with increasing the PBSA content. The variation trends in the values of  $t_{0.5}$ ,  $k$ , and  $1/t_{0.5}$  demonstrate that blending with PBSA retards the isothermal crystallization of PVDF since the former is actually in the melt during the crystallization of the latter and acts as a diluent.

The average values of the Avrami exponent  $n$  are around 2.5 for the isothermal crystallization of PVDF despite crystallization temperature and blend composition, indicating that the crystallization of PVDF might correspond to the spherulitic growth with heterogeneous nucleation. The almost unchanged  $n$  in the PVDF-rich blends indicates that the crystallization mechanism of PVDF does not change in the crystallization temperature range investigated in the present work irrespective of blend composition.

**Crystallization of Low- $T_m$  Component PBSA.** The spherulitic morphologies and crystallization kinetics of the low- $T_m$  component PBSA were also studied in its miscible blends with PVDF. Prior to the crystallization of PBSA, it is actually in the melt and miscible with the amorphous part of PVDF; therefore, PVDF/PBSA blends are miscible amorphous/crystalline polymer blends. PVDF/PBSA blends become crystalline/crystalline polymer blends after the crystallization of PBSA. Therefore, the crystallization of PBSA corresponds to the phase transition from amorphous/crystalline to crystalline/crystalline state according to the feature of the phase behavior of miscible crystalline/crystalline polymer blends.

Figure 5 shows the spherulitic morphologies of neat and blended PBSA crystallized at 70 °C. The spherulites in neat PBSA are compact, and the bundles of lamellae are few but thick (Figure 5a). In the case of the 20/80 blend, PVDF crystallizes first and fills the whole space after crystallization at 120 °C for 5 min; however, the birefringence of the PVDF crystals is weak (Figure 5b). On lowering the crystallization temperature to 70 °C, bright PBSA spherulites nucleate in the matrix of the PVDF spherulites and continue to grow until impinging on other PBSA spherulites. Compared with Figure 5a the presence of the PVDF crystals enhances the nucleation of PBSA as shown in Figure 5b. In the case of the crystallization of neat PBSA, the supercooling is so low that the nucleation is difficult at crystallization temperature 70 °C. For the crystallization of PBSA in a 20/80 blend at 70 °C followed by the crystallization of PVDF at 120 °C for 5 min, the tiny PVDF crystals formed first during the cooling process and the crystallization at 120 °C. The preexisting PVDF crystals may favor the nucleation of PBSA; therefore, the nucleation of PBSA is enhanced in the blends.

The overall crystallization kinetics of PBSA was studied by DSC for the PBSA-rich blends including 35/65, 20/80, and 0/100. In order to show the effect of blend composition on the crystallization of PBSA simply and directly, Figure 6 demon-

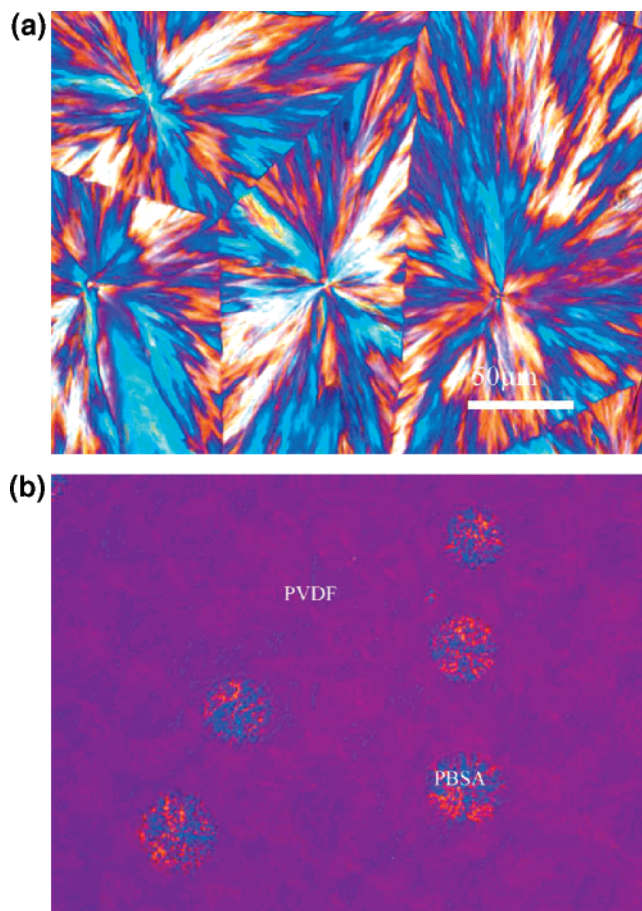


**Figure 5.** Spherulitic morphologies of PBSA (same magnification with bar = 50  $\mu\text{m}$ ): (a) neat PBSA at 70  $^{\circ}\text{C}$  for 20 min and (b) 20/80 blend at 70  $^{\circ}\text{C}$  for 6 min after crystallization of PVDF at 120  $^{\circ}\text{C}$  for 5 min.

strates the plots of relative crystallinity against crystallization time and the related Avrami plots for 0/100, 20/80, and 35/65 samples at 70  $^{\circ}\text{C}$ . The time for PBSA to finish crystallization in the blends is shorter than in neat PBSA (Figure 6a); furthermore, the crystallization time in the 20/80 blend is the shortest among the three samples. They show almost the parallel Avrami plots in Figure 6b, indicating the values of the Avrami exponent  $n$  are almost the same. All the related crystallization kinetics parameters are summarized in Table 2. The average values of  $n$  are around 2.6 for 0/100 and 20/80 blend, while they increase to around 2.8 for 35/65 blend. Roughly speaking, the Avrami exponent  $n$  of PBSA is not affected significantly by blending with PVDF. The average values of  $n$  are close to 3 in the PBSA-rich blends, indicating that the crystallization of PBSA may correspond to the spherulitic growth with heterogeneous nucleation. Moreover, in the above section PBSA is found to crystallize according to the spherulitic growth with heterogeneous nucleation as shown in the POM micrograph in Figure 5b. Therefore, it can be concluded that the DSC results are consistent with the POM morphology studies of PBSA in the previous section. The crystallization time becomes longer with increasing crystallization temperature despite blend composition. For a given blend composition, the values of  $t_{0.5}$  increase with increasing crystallization temperature, and the values of  $k$  and  $1/t_{0.5}$  decrease with the increase of crystallization temperature. The slowdown of the overall crystallization rate with increasing crystallization temperature may be attributed to the fact that nucleation becomes more difficult at high temperature for the PBSA-rich blends.

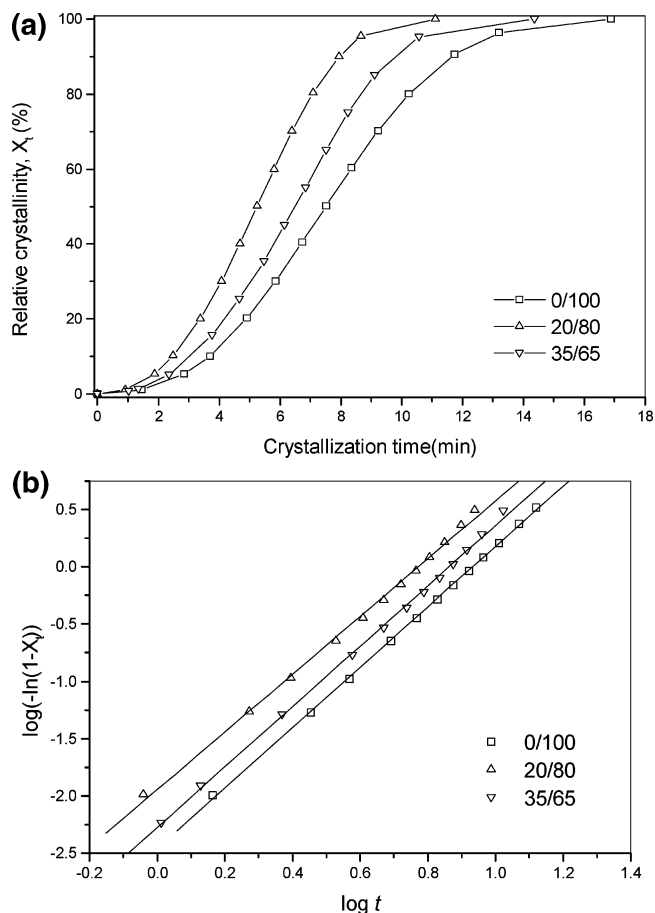


**Figure 6.** Effect of blend composition on the crystallization of PBSA at 70  $^{\circ}\text{C}$ : (a) development of relative crystallinity with crystallization time and (b) the Avrami plots.

However, the crystallization time becomes shorter for the blended PBSA at a given crystallization temperature, indicating that blending with PVDF accelerates the crystallization of PBSA in the blends. For a given crystallization temperature the values of  $t_{0.5}$  in the blends are smaller than that of neat PBSA. On the other hand, the values of  $k$  and  $1/t_{0.5}$  in the blends are larger than those of neat PBSA. The aforementioned results clearly show that the crystallization of PBSA is accelerated by the presence of the PVDF crystals in the blends. It should also be noted that the crystallization rate in 20/80 blend is the fastest at a given crystallization temperature. Figure 7 summarizes the effect of blend composition and crystallization temperature on the overall crystallization rate of PBSA for the PBSA-rich blends. The overall crystallization rate decreases with increasing crystallization temperature despite blend composition, indicating that crystallization temperature plays a dominant role of determining the overall crystallization rate for a given blend composition. However, the effect of blend composition on the overall crystallization rate of PBSA is somewhat complicated. The overall crystallization rate of the blends is larger than that of neat PBSA; furthermore, with further increasing the PVDF content the overall crystallization rate decreases. This kind of crystallization behavior must be related to the fact the crystallization of PVDF occurred before  $T_{c2}$  of PBSA was reached and PBSA must crystallize in the presence of the PVDF crystals.

The overall crystallization of PBSA is affected by the following factors. First, the presence of the PVDF crystals may have a positive effect on the nucleation of PBSA.<sup>5</sup> Thus, the overall crystallization rate may be increased due to the enhanced nucleation effect. The OM experiments confirmed the nucleation

Table 2. Crystallization Kinetic Parameters of PBSA for the PBSA-Rich Blends

PVDF/PBSA blends	$T_c$ (°C)	$n$	$k$ (min <sup>-n</sup> )	$t_{0.5}$ (min)	$1/t_{0.5}$ (min <sup>-1</sup> )
0/100	62	2.7	$3.03 \times 10^{-1}$	1.36	$7.34 \times 10^{-1}$
	64	2.5	$8.66 \times 10^{-2}$	2.28	$4.38 \times 10^{-1}$
	66	2.6	$2.40 \times 10^{-2}$	3.68	$2.72 \times 10^{-1}$
	68	2.7	$6.06 \times 10^{-3}$	5.71	$1.75 \times 10^{-1}$
	70	2.6	$3.49 \times 10^{-3}$	7.42	$1.35 \times 10^{-1}$
20/80	62	2.6	$8.35 \times 10^{-1}$	$9.31 \times 10^{-1}$	1.07
	64	2.6	$2.57 \times 10^{-1}$	1.47	$6.80 \times 10^{-1}$
	66	2.5	$1.02 \times 10^{-1}$	2.15	$4.65 \times 10^{-1}$
	68	2.6	$3.52 \times 10^{-2}$	3.12	$3.21 \times 10^{-1}$
	70	2.5	$1.13 \times 10^{-2}$	5.12	$1.95 \times 10^{-1}$
35/65	62	2.8	$5.62 \times 10^{-1}$	1.08	$9.28 \times 10^{-1}$
	64	2.7	$1.90 \times 10^{-1}$	1.62	$6.17 \times 10^{-1}$
	66	3.1	$4.24 \times 10^{-2}$	2.46	$4.07 \times 10^{-1}$
	68	3.0	$1.21 \times 10^{-2}$	3.91	$2.56 \times 10^{-1}$
	70	2.6	$5.32 \times 10^{-3}$	6.33	$1.58 \times 10^{-1}$

effect of the PVDF crystals. Second, the addition of PVDF to PBSA lowers the growth rate of the PBSA crystals due to a dilution effect which reduced the number of crystallizable units at the crystal growth front.<sup>5,8</sup> Third, the growth rate of the PBSA crystals reduces with increasing the PVDF content in the blends due to the physical restriction in the matrix of the PVDF crystals. The first factor accelerates the overall crystallization rate of PBSA, while the last two factors reduce the overall crystallization rate. Therefore, the overall crystallization rate of PBSA is a competitive result of enhanced nucleation and slower crystal growth rates in the PBSA-rich blends. The enhanced nucleation rate arisen from the presence of the PVDF crystals provides a reasonable explanation for the increase in the overall crystallization rate; therefore, the overall crystallization rates of 20/80 and 35/65 blends are larger than that of neat PBSA. Furthermore, the degree of crystallinity of PVDF formed at 120 °C would be a very important factor affecting the overall crystallization kinetics of PBSA. On the basis of the heat of fusion of 100% crystalline PVDF (93.2 J/g),<sup>5</sup> the degree of crystallinity of PVDF crystallized isothermally at 120 °C for 5 min was calculated from the crystallization exotherms and normalized with respect to the composition in the blend. The average values of degree of crystallinity of PVDF are around 47.3% for the 20/80 blend and 25.8% for the 35/65 blend. The degree of crystallinity in the 20/80 blend is as almost twice high as that in the 35/65 blend, which may have a significant positive effect on the nucleation of the later crystallization of PBSA at low crystallization temperatures. However, the further increase of PVDF also results in the decrease of the overall crystallization rate of PBSA; therefore, the overall crystallization rate of the 35/65 blend is smaller than that of the 20/80 blend.

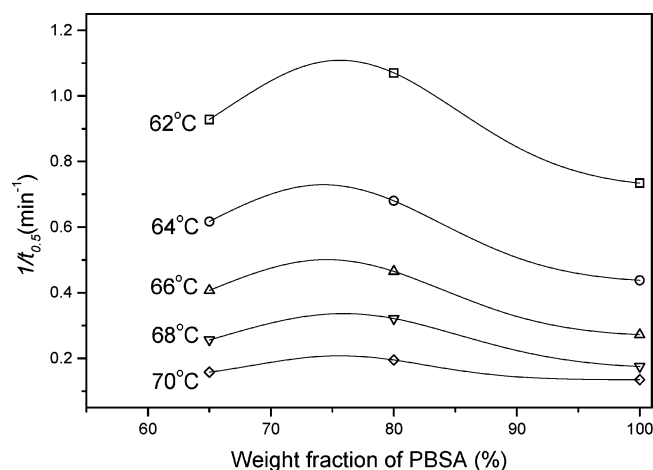


Figure 7. Temperature dependence of the overall crystallization rate of PBSA for the PBSA-rich blends.

Such decrease may be mainly due to the dilution effect, i.e., the addition of PVDF to PBSA reduced the number of crystallizable units at the crystal growth front. The physical constraints imposed by the previously crystallized PVDF might also contribute the decrease in PBSA crystallization kinetics for PVDF contents above 20%.

## Conclusions

PVDF/PBSA blends are miscible crystalline/crystalline polymer blends. PVDF and PBSA crystallize separately not simultaneously in the blends. Spherulitic morphologies and overall crystallization kinetics of PVDF/PBSA blends were studied by varying blend composition and crystallization conditions. The crystallization of PVDF corresponds to the phase transition from amorphous/amorphous to amorphous/crystalline state. Both the spherulitic growth rate and the overall crystallization rate of PVDF decrease with increasing crystallization temperature and the PBSA content in the blends; however, the crystallization mechanism does not change. PBSA actually acts as a diluent during the crystallization of PVDF. On the other hand, the crystallization of PBSA corresponds to the phase transition from amorphous/crystalline to crystalline/crystalline state, which is affected not only by blend composition and crystallization temperature but also strongly by the presence of the preexisting PVDF crystals. PBSA spherulites nucleate in the matrix of the PVDF spherulites and continue to grow until impinging on other PBSA spherulites. The overall crystallization rate of PBSA is accelerated in the blends. The presence of the preexisting PVDF crystals shows two opposite effects on the crystallization of PBSA. The presence of the preexisting PVDF crystals shows two opposite effects on the overall crystallization of PBSA, i.e., enhanced nucleation ability and slower crystal growth rates.

**Acknowledgment.** This work was financially supported by the National Natural Science Foundation, China (Grant No. 20504004), Program for New Century Excellent Talents in University, and the projects of Polymer Chemistry and Physics, BMEC (Grants Nos. XK100100433 and XK100100540). The authors thank the reviewers' critical comments and valuable suggestions to this manuscript.

## References and Notes

- (1) Avella, M.; Martuscelli, E. *Polymer* **1988**, *29*, 1731.
- (2) Marand, H.; Collins, M. *ACS Polym. Prepr.* **1990**, *31*, 552.
- (3) Chen, H. L.; Wang, S. F. *Polymer* **2000**, *41*, 5157.
- (4) Liu, A. S.; Liao, W. B.; Chiu, W. Y. *Macromolecules* **1998**, *31*, 6593.
- (5) Penning, J. P.; Manley, R. St. J. *Macromolecules* **1996**, *29*, 84.
- (6) Lee, J. C.; Tazawa, H.; Ikehara, T.; Nishi, T. *Polym. J.* **1998**, *30*, 327.
- (7) Qiu, Z.; Ikehara, T.; Nishi, T. *Polymer* **2003**, *44*, 2799.

- (8) Qiu, Z.; Fujinami, S.; Komura, M.; Nakajima, K.; Ikehara, T.; Nishi, T. *Polymer* **2004**, *45*, 4515.
- (9) Blümm, E.; Owen, A. J. *Polymer* **1995**, *36*, 4077.
- (10) Lee, J. C.; Tazawa, H.; Ikehara, T.; Nishi, T. *Polym. J.* **1998**, *30*, 780.
- (11) Ikehara, T.; Nishi, T. *Polym. J.* **2000**, *32*, 683.
- (12) Terada, Y.; Ikehara, T.; Nishi, T. *Polym. J.* **2000**, *32*, 900.
- (13) Hirano, S.; Nishikawa, Y.; Terada, Y.; Ikehara, T.; Nishi, T. *Polym. J.* **2002**, *34*, 85.
- (14) Ikehara, T.; Nishikawa, Y.; Nishi, T. *Polymer* **2003**, *44*, 6657.
- (15) Qiu, Z.; Ikehara, T.; Nishi, T. *Macromolecules* **2002**, *35*, 8251.
- (16) Ikehara, T.; Kimura, H.; Qiu, Z. *Macromolecules* **2005**, *38*, 5104.
- (17) Qiu, Z.; Yan, C.; Lu, J.; Yang, W.; Ikehara, T.; Nishi, T. *J. Phys. Chem. B* **2007**, *111*, 2783.
- (18) Hasegawa, R.; Takahashi, Y.; Chatani, Y.; Tadokoro, H. *Polym. J.* **1972**, *3*, 600.
- (19) Chatani, Y.; Hasegawa, R.; Tadokoro, H. *Polymer Prepr. Jpn.* **1971**, *20*, 420.
- (20) Ichikawa, Y.; Suzuki, J.; Washiyama, J.; Moteki, Y.; Noguchi, K.; Okuyama, K. *Polymer* **1994**, *35*, 3338.
- (21) Avrami, M. *J. Chem. Phys.* **1939**, *7*, 1193.

MA070255Y